

## NUMERICAL SIMULATION OF LABORATORY EXPERIMENTS ON THE ANALYSIS OF FILTRATION FLOWS IN POROELASTIC MEDIA

V.E. Borisov<sup>1</sup>

E.V. Zenchenko<sup>2</sup>

B.V. Kritsky<sup>1</sup>

E.B. Savenkov<sup>1</sup>

M.A. Trimonova<sup>1,2</sup>

S.B. Turuntaev<sup>2</sup>

narelen@gmail.com

zenchevj@gmail.com

boris.v.kritsky@gmail.com

e.savenkov@googlemail.com

trimonova.ma@gmail.com

s.turuntaev@gmail.com

<sup>1</sup>Keldysh Institute of Applied Mathematics, Russian Academy of Sciences,  
Moscow, Russian Federation

<sup>2</sup>Institute of Geosphere Dynamics, Russian Academy of Sciences,  
Moscow, Russian Federation

---

### Abstract

The work is devoted to mathematical simulation of laboratory experiments on the single-phase fluid displacement in synthetic porous samples. The basis of the mathematical model used is the system of poroelasticity equations in terms of the Biot's model, which implies that the processes of fluid filtration and the dynamics of changes in the stress-strain state of a continuous medium are considered together in the framework of a single coupled statement. For simulation, the software package developed at the Keldysh Institute of Applied Mathematics, Russian Academy of Sciences, was used. The laboratory experiments considered in this work were performed at the Institute of Geosphere Dynamics, Russian Academy of Sciences. The mathematical model used is briefly presented; the main computational algorithms and the features of their software implementation are described. A detailed description of the laboratory set-up, laboratory experiments themselves and their results are given. A significant part of the work is devoted to the problem statement description in terms of mathematical simulation. The results of calculations are presented; the calculated and experimentally observed dependencies are compared. The possible causes of the observed deviations are analyzed

### Keywords

*Poroelasticity, filtration, Biot's problem, laboratory experiment, simulation*

Received 16.07.2019

Accepted 09.09.2019

© Author(s), 2020

**Introduction.** The modern oil and gas field development is a complex process, the analysis of which cannot be imagined without appropriate mathematical simulation. Most studies are related to the development process optimization, which, one way or another, resolves into the problem of formation filtration simulation, the solution of which is necessary to assess the key characteristic, the formation productivity [1]. Typically, filtration type models are used to determine it, in which the mechanical state of the reservoir is taken into account approximately, for example, by setting the dependence of the formation porosity on the fluid pressure. However, a number of situations are known in which a correct description of the filtration processes requires a complete account of the medium stress-strain state. In particular, they include the hydraulic fracturing procedure [2], which involves pumping the fracturing fluid into the well under high pressure to create a highly permeable fracture, the presence of which leads to an increase in oil recovery. Such a process involves the simultaneous consideration of two problems: 1) formation fluid filtration; 2) fracture growth. To solve these problems correctly, it is necessary to couple the hydrodynamic problem with the geomechanical one. In this case, a poroelastic medium model is usually used to describe the formation — fluid system, which allows to describe fluid filtration in pores together with a full-fledged mechanical model of the formation stress-strain state. Models of this type were proposed by M. Biot [3].

When developing any numerical models, their verification is required. In the case of problems described above, obtaining data from real fields is a very complex and expensive procedure. Moreover, far from all the necessary data can be obtained. Therefore, the importance of laboratory experiments is increasing, for which most of the necessary technological parameters are known with higher accuracy.

In this work, we present the results of simulation two laboratory experiments conducted at the Institute of Geosphere Dynamics (IDG), Russian Academy of Sciences (RAS). Numerical calculations were performed using a software package designed to simulate three-dimensional processes of hydraulic fracture propagation, developed by the Keldysh Institute of Applied Mathematics RAS. The overall goal of the series of studies carried out: on the one hand, verification of the created program on model problems aimed at its further use for complex statements, and on the other hand — the refinement of the technique of performing laboratory experiments and the determination of the mathematical simulation methods required to describe them. The results of the filtration flow analysis in poroelastic media presented in this work are the first step toward realizing the specified goal, they were used to “calibrate” the

computational model for a laboratory set-up and determine the effective filtration parameters of the model.

**Laboratory set-up.** Laboratory experiments were carried out on a set-up developed at the IDG RAS [4, 5]. Its feature is the possibility of creating a three-dimensional stress-strain state in the sample necessary for conducting research on the processes associated with hydraulic fracturing, the instability of the propagation of fractures in injection wells, the interaction of several fractures with each other, etc. Features of the set-up, significant in terms of simulation the processes occurring in it, will be described below.

Structurally, the set-up consists of upper and lower metal covers, in the annular recess of which the side wall is fixed (Fig. 1, *a*, *b*). The covers are fastened together by 16 studs, which are not shown in the figure. The covers'

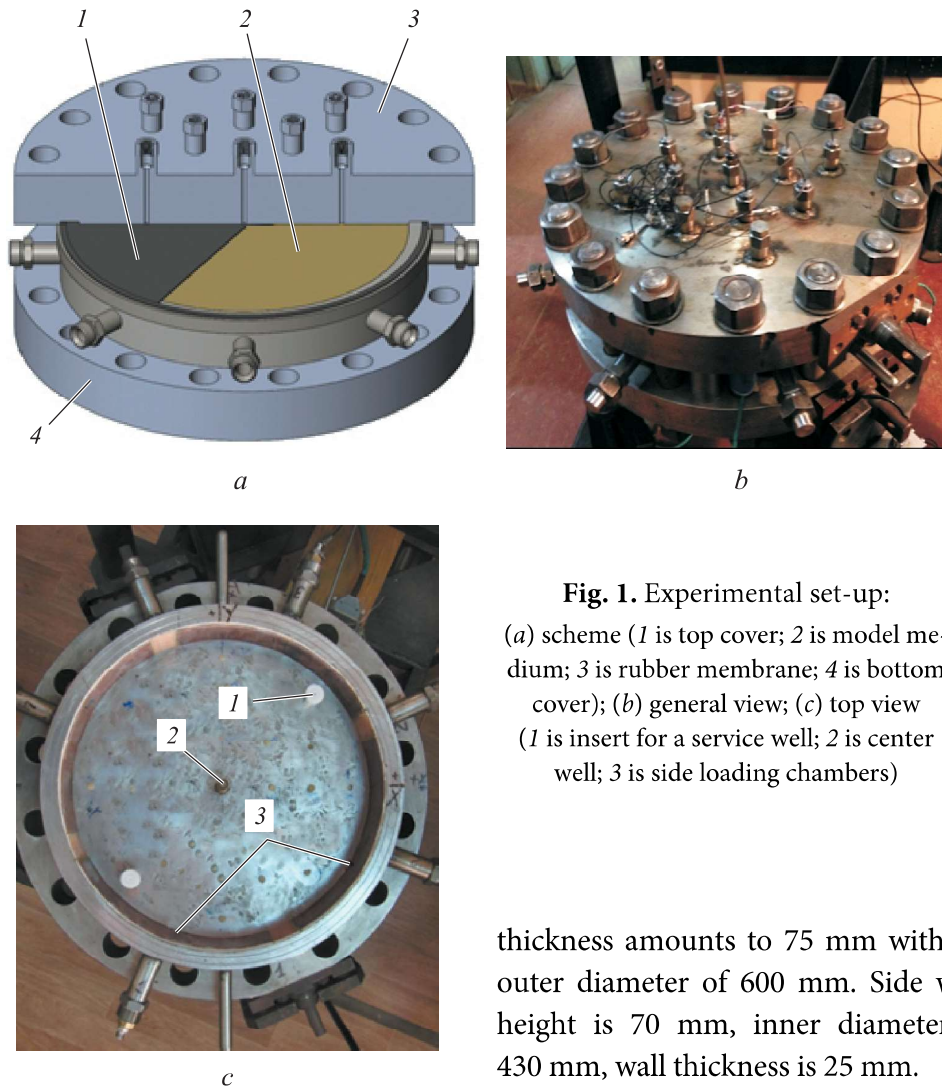


**Fig. 1.** Experimental set-up:  
 (a) scheme (1 is top cover; 2 is model medium; 3 is rubber membrane; 4 is bottom cover); (b) general view; (c) top view (1 is insert for a service well; 2 is center well; 3 is side loading chambers)

thickness amounts to 75 mm with an outer diameter of 600 mm. Side wall height is 70 mm, inner diameter is 430 mm, wall thickness is 25 mm.

The main parts of the set-up are made of corrosion-resistant steel. The covers are placed on the supporting frame, which allows to turnover them freely and to move the top cover into its bed. This makes it possible to perform the necessary operations related to the preparation and carrying out of experiments, despite the significant weight of the set-up components (the mass of the covers exceeds 160 kg). Before starting the experiment, material is poured into the set-up and after solidification it forms a model medium (sample).

The top cover is separated from the sample by a rubber membrane. A rubber ring and a clamp located around the perimeter of the membrane create a hermetically sealed space between the membrane and the cover. This space is filled with water under pressure, which allows simulation the lithostatic pressure in the reservoir model. The pressure above the membrane is maintained by means of a separation cylinder, the upper part of which is filled with compressed nitrogen at the required pressure, and the lower part with water. Horizontal loading of the model is ensured by sealed chambers located on the surface of the side wall (Fig. 1, c). The cameras are made of copper sheet 0.3 mm thick. The thickness of the inner cavity of the chambers is 3 mm, the height of the chamber is 68 mm. Arc length is approx. 80°. The chamber pipe extends from the side wall to the outside through a tight seal. The cameras are fixed on the side surface of the ring with silicone sealant. Side loading is carried out by injecting gas or liquid into the pairwise opposed chambers.

Technological through holes with a diameter of 6 mm equipped from the outside with welded threaded fittings were drilled in both covers and in the side wall. There are 29 holes in the top cover, 17 in the bottom one, and 6 in the side one. These holes can be used both for mounting various sensors and for fluid withdrawal or injection into the reservoir. The pore pressure in the model is measured through technological holes located in the bottom cover of the set-up, using strain gauges. The technological holes are water-filled and before pouring the material they are closed with foam rubber inserts that protrude 5 mm above the surface of the lower base and after filling the gypsum they are turned out to be mounted in it, ensuring the transfer of pore pressure to the strain gauges. The hole pattern is shown in Fig. 2.

Additionally, several wells can be formed in place of the technological holes, through which the saturated solution is subsequently pumped. When casting a sample, fluoroplastic inserts with a diameter of 15 mm are placed in it. After the material has hardened, the inserts are removed, and the formed wells are closed with fluoroplastic covers.

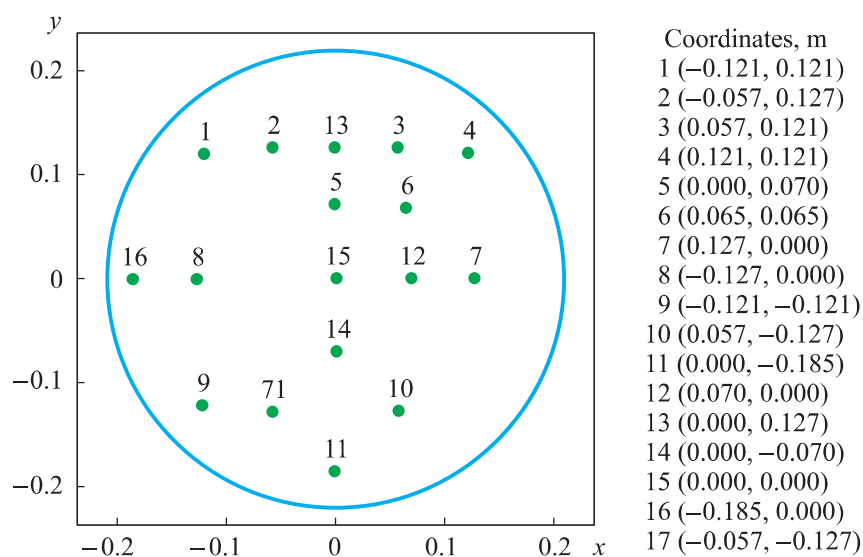


Fig. 2. The hole pattern on the bottom cover of the set-up

Laboratory experiments are carried out after drying of the material (usually on the third day from the moment of pouring). After assembling the experimental set-up, the model is loaded with a small vertical pressure (1 MPa), then the required pressure is set in the side chambers. Further, the vertical pressure is raised to the operating value. Before the experiment, the sample is additionally saturated with a liquid at a constant pump-in pressure of about 0.4 MPa at a technological injection well. The choice of a model medium is determined by the statement of the experimental problems to be solved and must be consistent with meeting that similarity criteria that are responsible for the possibility of transferring the experimental results to formation conditions [6], and with technological factors that make it possible to manufacture experimental samples in practice.

In this regard, for the class of problems under consideration, a gypsum-based mixture with Portland cement addition was selected. Good fluidity of the mixture and the absence of shrinkage during solidification allows for close contact with the set-up walls. To slow down the “setting” of gypsum, when preparing the mixture, citric acid at a concentration of 2 g/dm<sup>3</sup> is added to the water.

In the experiments discussed below, the model medium had the following properties: dynamic Poisson’s ratio  $\nu_{dyn} = 0.25$ , static Poisson’s ratio  $\nu_{st} = 0.2$ , dynamic Young’s modulus  $E_{dyn} = 7.5 \cdot 10^9$  Pa, static Young’s modulus  $E_{st} = 3.7 \cdot 10^9$  Pa, formation absolute permeability coefficient  $K = 2.4$  mD.

A description of the experiments to determine these strength and filtration characteristics of the sample can be found in Ref. [4, 5].

**Computational model.** Let the problem be solved in the spatial domain  $\Omega$ . The equations that make up the linear Biot's model in the case of a weakly compressible fluid have the form

$$\nabla \mathbf{T} + \rho \mathbf{g} = 0, \quad (1)$$

$$\frac{\partial}{\partial t}(m_f) + \nabla \left( -\rho_f \frac{k}{\mu} \nabla p \right) = 0, \quad (2)$$

where  $\mathbf{T} = \mathbf{T}' - b p \mathbf{I}$  is stress tensor,  $p$  is fluid pressure,  $\mathbf{T}' = \mathbf{C} : \mathbf{E}$  is effective stress tensor,  $\mathbf{C} = \text{const}$  is elastic coefficient tensor, for an isotropic medium  $\mathbf{C} = \lambda \mathbf{I} : \mathbf{I} + 2G \mathbf{I}$ ,  $\lambda, G$  are skeleton's Lamé coefficients,  $\mathbf{E}(\mathbf{u}) = [\nabla \otimes \mathbf{u} + (\nabla \otimes \mathbf{u})^T] / 2$  is linear strain tensor,  $\mathbf{u}(\mathbf{x}, t)$  is displacement vector;  $\rho$  is sample density;  $\mathbf{g} = g \mathbf{e}_g$ ,  $g$  is acceleration of gravity,  $\mathbf{e}_g$  is gravity direction vector;  $m_f$  is fluid mass per unit volume of saturated medium,  $m_f = \rho_f^0 v_f$ ,  $v_f = b \varepsilon + \frac{1}{M} p$ ,  $\varepsilon = \mathbf{E} : \mathbf{I}$ ,  $b = \text{const}$ ,  $M = \text{const}$  are Biot's parameters,  $\rho = \text{const}$  is saturated medium density,  $\rho = \rho_s^0 (1 - \varphi_0) + \rho_f^0 \varphi_0$ ,  $\rho_s^0 = \text{const}$  is skeleton density,  $\rho_f^0 = \text{const}$  is fluid density,  $\varphi_0 = \text{const}$  is initial porosity,  $\Delta \rho_f / \rho_f^0 = \Delta p / K_f$  is constitutive relation for weakly compressible fluid,  $K_f$  is bulk compression modulus of fluid;  $k = \text{const}$  is porous medium permeability coefficient;  $\mu$  is fluid viscosity [6].

The statement of the problem should be supplemented by the boundary conditions at the boundary of the  $\Omega$  region, as well as the initial conditions at the time instant  $t = 0$ . For the "elastic" part of the problem (Eq. (1)), components of (total) normal stresses or components of the displacement field can be specified on the boundary of the region. For the "filtration" part of the problem (Eq. (2)), pressure values or the normal component of the fluid mass flux vector can be specified. The primary unknowns of the problem are the displacement field of the host medium  $\mathbf{u}$  and the fluid pressure in the formation  $p$ .

To numerically solve the system of poroelasticity equations (1), (2), we use one of the versions of the finite element method *X-FEM* [7], which allows to take into account the presence of discontinuities associated with a crack in the medium. To approximate the equations in time, the implicit Euler method is used, and a special iterative algorithm between groups of filtration and elasticity

equations is used to determine the solution of the complete system. A more detailed description of the numerical method used in the work can be found in Ref. [8].

The software package is implemented as a compute kernel in C++11 and an interface in *Python* under OS *Linux*. To link C++ and *Python*, the *SWIG* tool [9] is used. When developing the complex, the *aiwlib* library [10] was widely used. To solve systems of linear algebraic equations, a *gmm++* library [11] is used. Since it is possible to model many different problem statements with one compute kernel, a separate *Python* head script is created for each statement, which contains the instantiating a model event class, its initialization, a calculation timing loop and uploading calculation results. To set the computational domain of complex geometry and generate an unstructured mesh, the widely used *Salome* package [12] is utilized, which allows the use of various meshing algorithms. For the purposes of this work, the *NETGEN* mesh generator [13] was used. An example of the created geometry of the sample and the corresponding grid for the calculation is presented in Fig. 3.

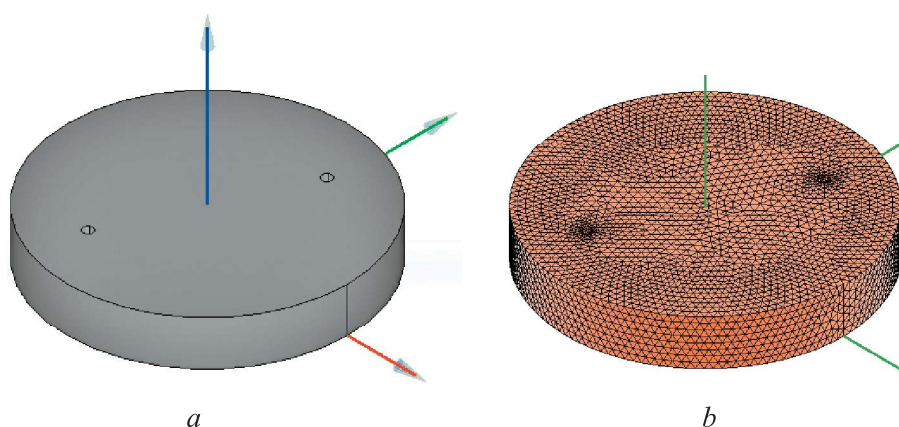


Fig. 3. Example of sample geometry (a) and mesh (b) in *Salome*

**Experiment results.** For numerical simulation of the experimental set-up operation, a number of parameters should be set, for example, the Biot's module, for the determination of which additional laboratory experiments are needed to be carried out that require special equipment. In this work, we used the parameter values taken from [14], where similar materials and mixtures were used. Obviously, with this approach, some "calibration" of the mathematical model parameters is necessary to correctly describe the experimental set-up operation. To this end, we used the results of two similar laboratory experiments to determine the pressure build-up and drawdown

curves as a function of time. To do this, after saturating the sample, gypsum solution was pumped to create a stationary pore pressure field in it, then the pressure in the injection well was released, it was “sealed”, and the producing well continued to work. Accordingly, the pressure value recorded in the sensors first increased, and then dropped. The temporal dynamics of this change was recorded during the experiment.

In the first experiment, wells were installed in holes 3 and 17, in the second one wells installed in holes 4 and 9 (see Fig. 2), pressure sensors were placed in holes 1, 2, 4–7, 10–16 (the measured pressure corresponded to the pressure at a distance 5 mm from the bottom of the sample). After the installation of wells and sensors, gypsum was poured into the set-up and dried for 2–3 days. Next, a pressure  $P_{top}$  simulating lithostatic pressure was applied to the sample from above. At the same time, pressure was not set in the side chambers. Then, gypsum solution with constant pressure  $P_{inj}$  was pumped into one of the wells. Another well is connected to the atmosphere. According to the design of the experiment, the saturation of the sample continued until a steady-state regime was established in it. The establishment was determined by stabilizing the flow rate in the producing well, after which the solution feeding was stopped. The pressure values in the sensors were recorded throughout the experiment every 0.01 s.

To numerically solve the system of Eq. (1) and (2), it is necessary to set the boundary conditions corresponding to the experiment. A schematic view of a sample with applied loads is shown in Fig. 4. For the elastic part of the problem, the boundary conditions were set as follows. A vertical load was set on the upper surface of the sample: the vector of the applied force is equal to the normal

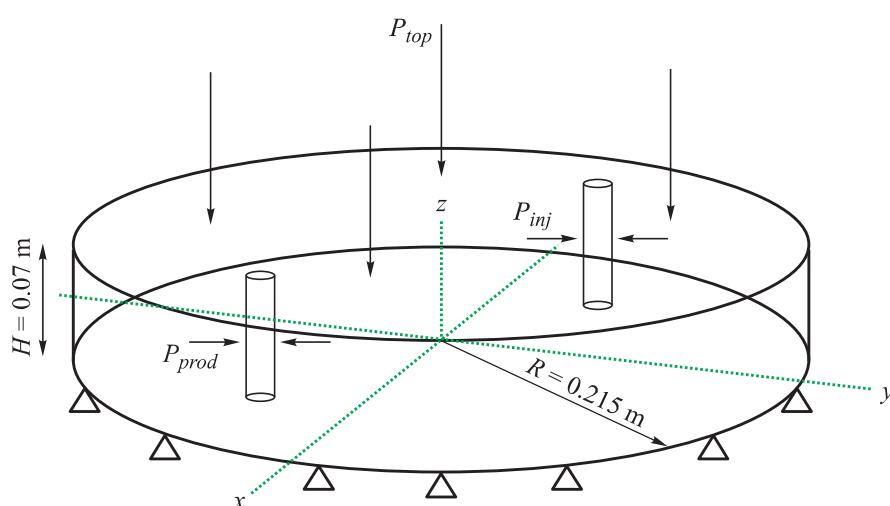


Fig. 4. Schematic view of a sample with applied loads



component  $\mathbf{f} = \mathbf{f}_n = P_{top}\mathbf{n}$ . The lower boundary of the sample is rigidly fixed vertically; therefore, a boundary condition for moving along the axis  $OZ$ :  $u_z = 0$  was placed on it. To exclude the rotation of the sample around its axis and the shift of the sample in the plane  $OXY$ , the boundary condition was set on the side surface of the sample in the form of zero tangential displacement in the plane  $OXY$ :  $\mathbf{u} \cdot \mathbf{e}_\tau = 0$ , where  $\mathbf{u} = (u_x, u_y, u_z)$ ,  $\mathbf{e}_\tau = (-n_y, n_x, 0)$ , i.e.,  $-n_y u_x + n_x u_y = 0$ . Normal stresses were set on the surface of the wells:  $T_n = P_{inj}$  for injection well and  $T_n = P_{prod}$  for producing one. After injection was stopped at the second stage of the experiment, the stress on the side surface of the producing well was set based on the local pressure in the adjacent pore medium.

For the filtration part of the system, the impermeability boundary conditions  $\partial P / \partial \mathbf{n} = 0$  were set on the upper, lower, and side surfaces of the sample. At the first stage of the calculation, constant pressures were set at the wells: a solution was pumped into the injection well under pressure  $P_{inj}$ , and the producing well was connected with the atmosphere,  $P_{prod} = 1$  atm. After reaching the conditions for switching the mode, the pumping of the solution into the injection well was stopped and the impermeability condition was set on it.

*Experiment 1.* During experiment 1, the following parameters were set:  $P_{prod} = 1$  atm;  $P_{inj} = 14.5$  atm;  $P_{top} = 20$  atm;  $1 \text{ atm} = 101\,325 \text{ Pa}$ . The injection well with a radius of 7.5 mm was located in hole 3, the producing well was located in hole 17.

As stated above, the pressure in the sensors must first increase, and then gradually decrease. When analyzing the results, it turned out that the initial process of maintaining a constant pressure in the well is unstable. Therefore, for comparison with the numerical solution, only the second stage of the experiment was used, i.e., the process of pressure decrease. It should be noted that in the laboratory experiment the stationary state was not reached, therefore the shut-off of the injection well in numerical calculation was carried out at the moment of reaching the known threshold pressure value on the central sensor.

The first comparison of the numerical simulation results and experimental data showed their cardinal discrepancy in the rate of pressure drop (Fig. 5). This happened for several reasons. First, for the calculations, we used the Biot's parameter values taken from [14], which corresponded to the filtration of a saturated solution through cement paste. Obviously, for this experiment, they provided only a qualitative agreement between the results. Secondly, as additional studies have shown, after solidification, the sample contains residual air, which interferes with the filtration process. To take this effect into account,

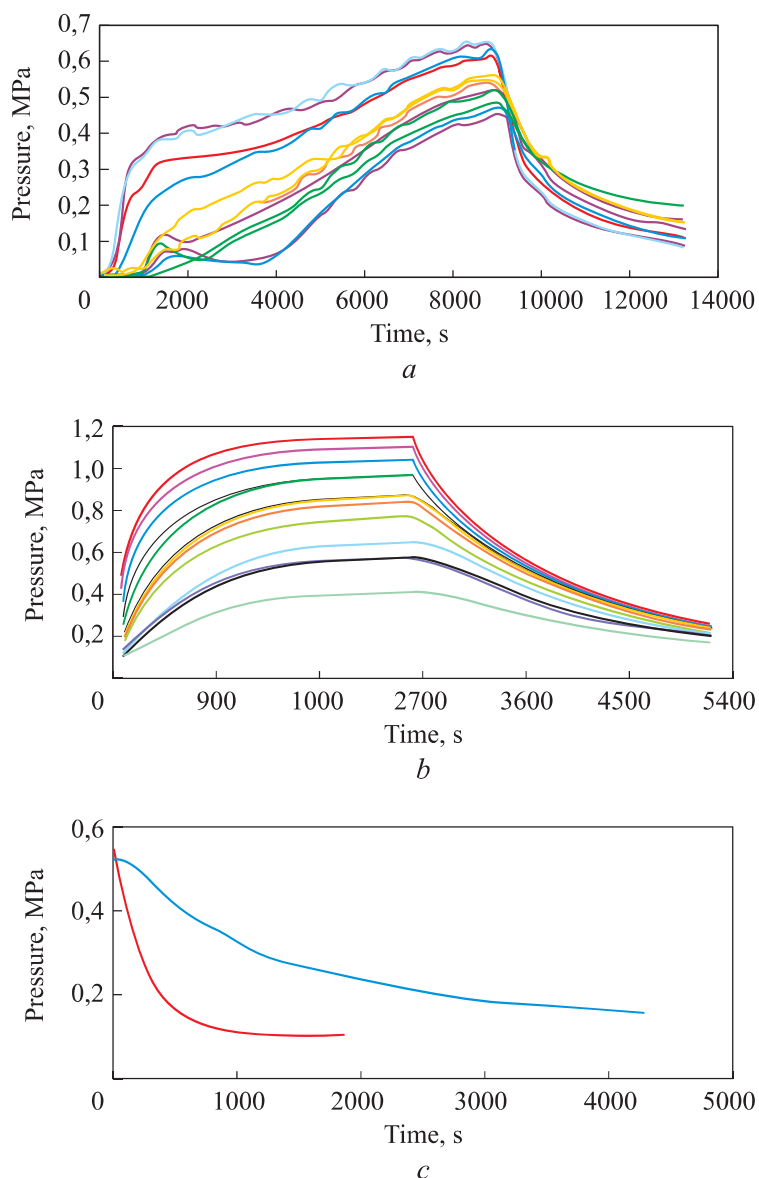


**Fig. 5.** Initial comparison of pressure draw-down curves obtained in experiment and simulation:

*a* is experimental curves; *b* is preliminary simulation data; *c* is pressure drop on one of the sensors (blue curves belongs to experiment, red belongs to calculation)

the parameters of the mixture of the poroelastic medium (skeleton) + air were corrected according to the Hashin — Shtrikman method [15], which allows to strictly determine the upper and lower estimates of elastic media for a two-phase material. In particular, the formula for the compression module of a composite medium is written as follows:

$$K_{HS}^{\pm} = K_2 + \frac{\alpha_{HS}}{(K_1 - K_2)^{-1} + (1 - \alpha_{HS}) \left( K_2 + \frac{4}{3} \mu_2 \right)^{-1}}, \quad (3)$$

where  $K_{1,2}$ ,  $\mu_{1,2}$  are compression and shear modules of constituent materials;  $\alpha_{HS}$  is specific content of one of the constituents. Here the upper boundary is calculated when  $K_2 > K_1$ , the lower one — vice versa.

In this work, the following sequence of actions when calculating the effective properties of the medium is used.

1. Determination of the specific air content in the skeleton + air mixture from the known porosity of the sample  $\varphi$  and the air fraction  $\alpha$  in the pore space:

$$\alpha_{HS} = \frac{\alpha\varphi}{(1 - \varphi) + \alpha\varphi}.$$

2. Calculation of the skeleton compressibility using the known Biot's coefficient  $b$  and bulk compression modulus of the sample  $K$ :

$$K_s = \frac{K}{1 - b}.$$

3. Calculation of the upper and lower estimates of the skeleton + air mixture compressibility  $K_{s,air}^{\pm}$  according to the Hashin — Shtrikman formula (3).

4. Calculation of the upper and lower estimates of the Biot's module of the skeleton + air mixture  $M^{\pm}$  during filtration of the gypsum solution with compressibility  $K_f$ :

$$\frac{1}{M^{\pm}} = \frac{b - \varphi}{K_{s,air}^{\pm}} + \frac{\varphi}{K_f}.$$

5. Determination of the volume fraction of the solution in a saturated skeleton + air / solution medium by the known porosity of the sample and the air fraction in the pore space.

6. Calculation of the upper and lower estimates of the skeleton + air / solution material compressibility according to the Hashin — Shtrikman formula (3).

7. Calculation of effective elastic parameters of the medium (Young's modulus, Poisson's ratio) from the effective compressibility value and the initial value of the shear modulus of the poroelastic medium, which is not affected by the presence of air.

The estimates found for the skeleton + air material compressibility amounted to  $10^6$  and  $10^{10}$  Pa for the lower and upper boundaries, respectively. Similar estimates are valid for the Biot's module, whose change is decisive for the filtration-volumetric characteristics of the medium. In particular, with a Biot's modulus of the order of  $10^7$ – $10^8$  Pa, the filtration rates obtained in the laboratory experiment and numerical simulation provide an acceptable coincidence of the pressure curves (Fig. 6). Variation of the elastic moduli, as expected, did not have a significant effect.

Thus, the simulation performed demonstrated the possible significant effect of air trapped in the sample on the filtration process. For a more accurate analysis, another laboratory experiment was conducted with a confirmed establishment of a stationary mode in order to eliminate error associated with the uncertainty of meeting the criterion of changing the operation of the injection well.

*Experiment 2.* The scheme of experiment 2 on the whole duplicates the one for experiment 1. The differences that are significant in terms of mathematical simulation consist, firstly, in changing the location of operating wells (the injection well is placed in hole 9, and the producing one is placed in hole 4), and secondly, in changing the pressure  $P_{inj} = 4.2$  atm and the vertical load  $P_{top} = 12$  atm. The boundary conditions were set similarly to experiment 1 with the necessary corrections for the changed input data. In particular, when analyzing the results of the laboratory experiment, it was found that the pressure decreases to not 1 atm, as could be expected from the experimental conditions, but to 1.5 atm. This led to a change in the corresponding boundary condition for the producing well. The switching of the operating mode of the injection well was performed when a stationary flow pattern was achieved in the sample.

The results of comparing the pressure curves obtained in experiment 2 and during simulation are shown in Fig. 7 for each sensor. On the part of the experimental data, there is noise with a clear-cut boundary, which acceptably coincides with the numerical results. However, a slight discrepancy in the rate of pressure change observed at the initial stage of simulation is noticeable. Most likely, one of the reasons is the presence of residual air in the sample, which is displaced for some time by the action of the pumped solution at the beginning of the experiment. This hypothesis is based on the observation that during the experiment, the fluid did not start to flow out immediately after the start of the fluid pumping into the injection well, which indicates undersaturation of the sample. Another reason may be the manifestation of the viscoelastic and plastic properties of gypsum at the initial stage of displacement.

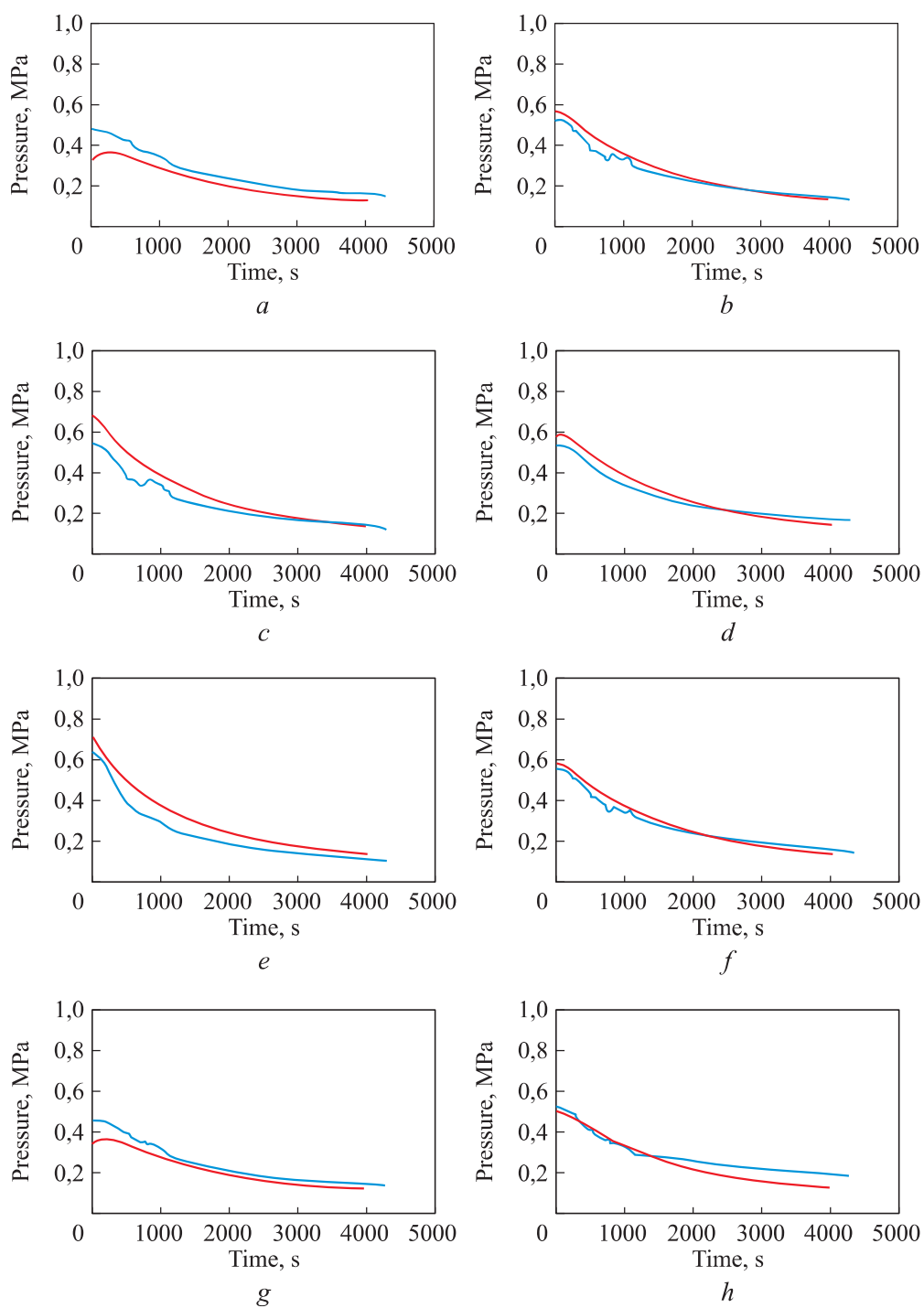


**Fig. 6.** Comparison of pressure curves obtained in the experiment (blue) and simulation (red) for sensors 12 (*a*), 2 (*b*), 13 (*c*), 5 (*d*), 4 (*e*), 14 (*f*), 15 (*g*), 16 (*h*)

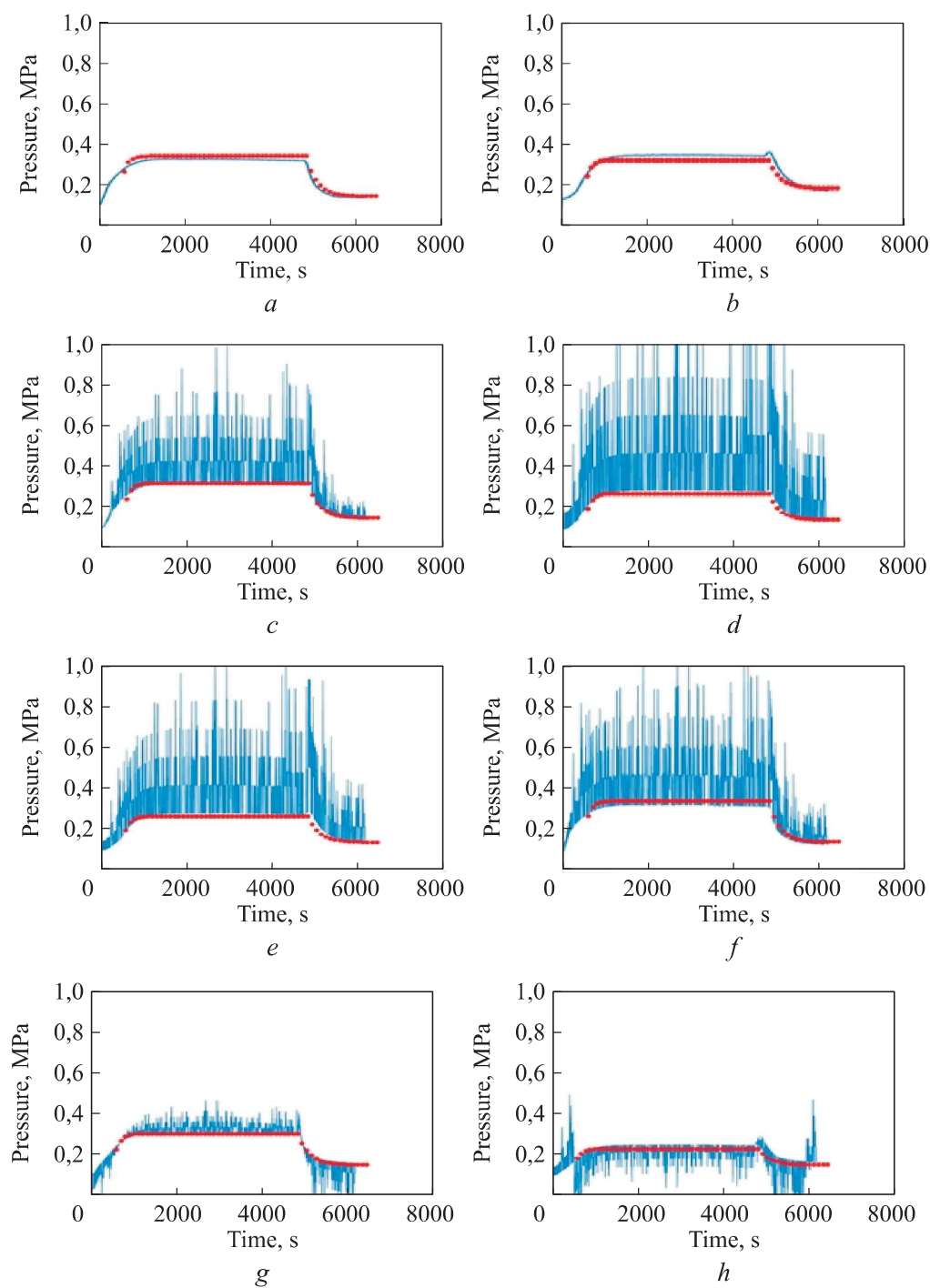


**Fig. 7.** Comparison of pressure curves obtained in the experiment (blue curves) and simulation (red curves) for sensors 8 (*a*), 7 (*b*), 10 (*c*), 2 (*d*), 5 (*e*), 11 (*f*), 1 (*g*), 3 (*h*)

**Conclusion.** The application of numerical simulation for the analysis of laboratory experiments conducted at the IDG RAS. Numerical calculations were performed using a software package designed for simulation three-dimensional processes of hydraulic fracture propagation, developed at Keldysh Institute of Applied Mathematics RAS. The presented results on the analysis of filtration flows in poroelastic media made it possible to compare the data of laboratory and numerical experiments, to determine some of the unknown parameters for the numerical model necessary for further analysis of laboratory experiments in more complex statements. In particular, the effective filtration parameters of the model were determined using the Hashin — Shtrikman method, which allowed to obtain an acceptable agreement between the results of laboratory experiments and numerical simulation.

## REFERENCES

- [1] Aziz Kh., Settari A. Petroleum reservoir simulation. Applied Science Publ., 1979.
- [2] Economides M.J., Oligney R.E., Valko P. Unified fracture design: bridging the gap between theory and practice. Orsa Press Alvin, 2001.
- [3] Biot M.A. General theory of three-dimensional consolidation. *J. Appl. Phys.*, 1941, vol. 12, iss. 2, pp. 155–164. DOI: <https://doi.org/10.1063/1.1712886>
- [4] Trimonova M., Baryshnikov N., Zenchenko E., et al. Study of the unstable fracture propagation in the injection well: numerical and laboratory modeling. *SPE Russ. Petroleum Technology Conf.*, doc. 187822-MS. DOI: <https://doi.org/10.2118/187822-MS>
- [5] Trimonova M., Zenchenko E., Baryshnikov N., et al. Estimation of the hydraulic fracture propagation rate in the laboratory experiment. In: Karev V., Klimov D., Pokazeev K. (eds). *Physical and Mathematical Modeling of Earth and Environment Processes. PMMEEP 2017*. Springer Geology. Springer, Cham, 2018, pp. 259–268. DOI: [https://doi.org/10.1007/978-3-319-77788-7\\_27](https://doi.org/10.1007/978-3-319-77788-7_27)
- [6] de Pater C.J., Cleary M.P., Quinn T.S., et al. Experimental verification of dimensional analysis for hydraulic fracturing. *SPE Production & Facilities*, 1994, vol. 9, iss. 4, pp. 230–238. DOI: <https://doi.org/10.2118/24994-PA>
- [7] Borisov V., Ivanov A., Ramazanov M., et al. Poroelastic hydraulic fracture simulation using X-FEM/CPF approach. In: Karev V., Klimov D., Pokazeev K. (eds). *Physical and Mathematical Modeling of Earth and Environment Processes (2018)*. Springer Proceedings in Earth and Environmental Sciences. Cham, Springer, 2019, pp. 323–333. DOI: [https://doi.org/10.1007/978-3-030-11533-3\\_32](https://doi.org/10.1007/978-3-030-11533-3_32)
- [8] Borisov V.E., Ivanov A.V., Kritsky B.V., et al. Numerical simulation of poroelasticity problems. *Preprinty IPM im. M.V. Keldysha* [KIAM Preprint], 2017, no. 81, 36 p. (in Russ.). DOI: <https://doi.org/10.20948/prepr-2017-81>
- [9] <http://www.swig.org/>: website (accessed: 15.04.2019).

- [10] Ivanov A.V., Khilkov S.A. Aiwlib library as the instrument for creating numerical modeling applications. *Nauchnaya vizualizatsiya* [Scientific Visualization], 2018, vol. 10, no. 1, pp. 110–127 (in Russ.). DOI: <https://doi.org/10.26583/sv.10.1.09>
- [11] <http://getfem.org/gmm.html>: website (accessed: 15.04.2019).
- [12] <https://www.salome-platform.org/>: website (accessed: 15.04.2019).
- [13] <https://ngsolve.org/>: website (accessed: 15.04.2019).
- [14] Constantinides G., Ulm F.J. Multi-scale poroelastic properties of cement-based materials. *FraMCoS-5 Vail*. At Vail, Colorado, USA, pp. 1–9.
- [15] Hashin Z., Shtrikman S. A variational approach to the theory of the elastic behaviour of multiphase materials. *J. Mech. Phys. Solids*, 1963, vol. 11, iss. 2, pp. 127–140. DOI: [https://doi.org/10.1016/0022-5096\(63\)90060-7](https://doi.org/10.1016/0022-5096(63)90060-7)

**Borisov V.E.** — Cand. Sc. (Phys.-Math.), Research Fellow, Keldysh Institute of Applied Mathematics, Russian Academy of Sciences (Miuskaya ploschad 4, Moscow, 125047 Russian Federation).

**Zenchenko E.V.** — Senior Research Fellow, Institute of Geosphere Dynamics, Russian Academy of Sciences (Leninskiy prospekt 38/1, Moscow, 119334 Russian Federation).

**Kritsky B.V.** — Junior Research Fellow, Keldysh Institute of Applied Mathematics, Russian Academy of Sciences (Miuskaya ploschad 4, Moscow, 125047 Russian Federation).

**Savenkov E.B.** — Cand. Sc. (Phys.-Math.), Leading Researcher, Keldysh Institute of Applied Mathematics, Russian Academy of Sciences (Miuskaya ploschad 4, Moscow, 125047 Russian Federation).

**Trimonova M.A.** — Junior Research Fellow, Keldysh Institute of Applied Mathematics, Russian Academy of Sciences (Miuskaya ploschad 4, Moscow, 125047 Russian Federation); Junior Research Fellow, Institute of Geosphere Dynamics Russian Academy of Sciences (Leninskiy prospekt 38/1, Moscow, 119334 Russian Federation).

**Turuntaev S.B.** — Dr. Sc. (Phys.-Math.), Director of Institute of Geosphere Dynamics, Russian Academy of Sciences, Head of Laboratory of Geomechanics and Fluid Dynamics, Institute of Geosphere Dynamics, Russian Academy of Sciences (Leninskiy prospekt 38/1, Moscow, 119334 Russian Federation).

**Please cite this article as:**

Borisov V.E., Zenchenko E.V., Kritsky B.V., et al. Numerical simulation of laboratory experiments on the analysis of filtration flows in poroelastic media. *Herald of the Bauman Moscow State Technical University, Series Natural Sciences*, 2020, no. 1 (88), pp. 16–31. DOI: <https://doi.org/10.18698/1812-3368-2020-1-16-31>